In Vivo Contact Stresses during Activities of Daily Living after Knee Arthroplasty

Darryl D. D'Lima,[1] Nikolai Steklov,[1] Benjamin J. Fregly,[2,3,4] Scott A. Banks,[2,3,4] Clifford W. Colwell Jr.[1]

[1]Shiley Center for Orthopaedic Research and Education at Scripps Clinic, 11025 North Torrey Pines Road, Suite 140, La Jolla, California 92037, [2]Department of Mechanical and Aerospace Engineering, University of Florida, Gainesville, Florida,[3] Department of Orthopaedics and Rehabilitation, University of Florida, Gainesville, Florida,[4] Department of Biomedical Engineering, University of Florida, Gainesville, Florida

Received 30 October 2007; accepted 25 February 2008
Published online in Wiley InterScience (www.interscience.wiley.com). DOI 10.1002/jor.20670

ABSTRACT: We implanted an electronic knee prosthesis to measure tibial forces in vivo during activities of daily living after total knee arthroplasty. We used tibial forces and knee kinematic data collected in vivo to calculate contact stresses using finite element analysis. The polyethylene insert was modeled as an elastoplastic material, and predicted contact stresses were validated using pressure sensitive sensors. Peak contact stresses generated during walking were similar but about 18% lower than those calculated for International Standards Organization (ISO)-recommended wear simulation conditions. Stair climbing generated higher contact stresses (32 MPa) than walking (26 MPa). However, both high flexion activities (lunge and kneel) generated even higher contact stresses, with the lunge activity generating the highest stresses (56 MPa). The activities that generated high contact stresses also resulted in high equivalent plastic strain. However, the lunge activity generated dramatically higher plastic equivalent strain than the other activities. In vivo measurement of kinematics, forces, and contact stresses may be used to develop more clinically relevant wear simulator protocols. Contact stresses generated during high flexion activities were substantially higher and were largely due to the reduced contact area in deep flexion rather than due to an increase in contact forces. Our results support the use of "high flexion" designs that improve contact conditions and preserve contact area at high flexion angles. © 2008 Orthopaedic Research Society. Published by Wiley Periodicals, Inc. J Orthop Res, 2008

Keywords: total knee arthroplasty; tibial forces; knee forces; contact stresses; finite element analysis

Polyethylene remains the most popular bearing material for total knee arthroplasty (TKA). Despite its widespread use, wear and damage continue to be major factors implicated in revisions.[1] The yield strength of polyethylene ranges from 13 to 32 MPa[2–4]; even lower values are reported for fatigue strength.[5] Polyethylene contact stresses often exceed the yield strength.[6–9] The contact area of a natural knee ranges from 765 to 1150 mm^2, but drops to 80 to 300 mm^2 after TKA, depending on the load and design.[10–12] Peak contact stresses have been reported as high as 30–60 MPa.[8,9] These studies have been either computed using mathematical models or measured in vitro with pressure sensors under estimated knee forces. Tibiofemoral forces measured in vivo would be extremely useful in evaluating these reports.

Contact stress and sliding distance are the major factors influencing polyethylene wear.[13–17] However, in vivo contact stresses after TKA have yet to be measured. A validated method of computing in vivo contact stresses from measured tibiofemoral contact force would therefore be very valuable, since in vivo contact forces and stresses could be used to develop and validate clinically relevant in vitro and in silico wear simulations.

Knee wear simulators can be classified into two categories: predominantly force-controlled[18,19] and predominantly displacement-controlled[20,21] machines. In both types, the vertical load is directly controlled. Both types have advantages and disadvantages. Displacement-controlled simulators directly manipulate the relative position of the femoral and tibial components using kinematic data and are therefore easier to model, since knee kinematics are easily measured in vivo. However, the forces generated may vary from in vivo conditions due to differences in implant alignment and lack of soft-tissue constraints. Further, direct comparisons between implants of different designs may be invalid. Force-controlled simulators apply forces in the anteroposterior (AP) direction and moments about the superoinferior direction to achieve relative motion (although flexion is typically displacement-controlled). However, the force magnitudes and directions have not yet been validated by in vivo measurements. The International Standards Organization (ISO) standards for knee wear simulation are widely used, but the type and magnitude of wear produced is typically benign and is not considered representative of wear observed on retrievals.[7,22] In addition, the ISO standard represents a walking cycle; other activities that may affect wear, such as stair climbing and deep flexion activities, are not included.

We implanted an instrumented knee prosthesis, which we used to measure tibial forces in vivo during activities of daily living after TKA.[22–25] We also used in vivo-measured tibiofemoral forces and kinematics to compute the mediolateral distribution of contact forces and the relationship between the external knee adduction moment and medial contact force using an elastic foundation contact model.[26,27] In the present study, we used the same dataset to calculate in vivo contact stresses using a validated finite element (FE) model. In vivo contact stresses are largely associated with wear and damage. Therefore, our primary aim was to rank activities of daily living based on the potential for wear

Correspondence to: Darryl D. D'Lima (T: 858-332-0166; F: 858-332-0140; E-mail: ddlima@scripps.edu)

and damage (using contact stress as a marker). Our secondary objective was to compare the contact stresses and sliding distances calculated from in vivo data with those generated using the ISO-recommended wear simulation.

METHODS

Measurement of Knee Kinematics and Forces

A 68-kg, 80-year-old male with primary osteoarthritis of the knee was implanted with a tibial prosthesis instrumented with force transducers, a power induction coil, a microtransmitter, and an antenna.[24] An external coil was used to generate power in the internal coil, which powered the force transducers and the microtransmitter (see D'Lima et al.[25]). The total axial load and the location of center of pressure were recorded for level walking, stair climbing, kneeling, and deep knee bend (lunge) activities, 8 months postoperative.[26] Knee kinematics were measured using a validated fluoroscopic analysis technique.[28]

Finite Element Model

An FE model was constructed using commercial software (Fig. 1, MSC.MARC, MSC.Software, Santa Ana, CA). The femoral component and tibial tray were modeled as rigid bodies. The insert was meshed with hexahedral and pentahedral elements. Contact was detected when the perpendicular distance between the femoral surface and a node on the insert was <0.01 mm. When contact was detected, direct constraints were placed on the motion using boundary conditions at the contacting nodes. Optimum mesh density was calculated in two stages. Predicted peak contact stresses and contact area in a simplified model of a spherical rigid body indenter with a radius of 14 mm (simulating a femoral condyle) contacting a flat "insert" ($100 \times 100 \times 100$ mm) with a linear elastic modulus of 1000 MPa were compared with an analytic Hertzian contact solution.[29] Multiple loads (from 100 to 1000 N) generating peak contact stresses of up to 70 MPa were simulated. Convergence of contact area measurement and peak contact stresses within 3% of the analytical solution was achieved using elements with a mean edge length of 0.25 mm. Next, convergence of peak contact stresses for the FE model using prosthetic component geometry was obtained with a mean edge length of 0.25 mm (<1% change in peak contact stresses between mean element sizes of 0.5 and 0.25 mm).

Polyethylene was modeled as a nonlinear elastoplastic material using von Mises yield criteria.[30] Below the von Mises yield point, the material behaved in a purely elastic manner. Beyond yield, the material exhibited strain-hardening behavior. The true stress–strain behavior in uniaxial tension and compression including the yield criterion were obtained from published data.[30] Contact stresses and contact area were computed for level walking, stair climbing, and for static high flexion activities (kneeling and lunge) as described below.

Model Validation

For validation, the predicted contact measures (peak stresses and contact area) were compared with those experimentally measured using K-Scan sensors (Tekscan, South Boston, MA). The sensors consisted of plastic laminated, thin-film (nominally ~100 μm thick) electronic pressure transducers with two 9.2 cm^2 sensing arrays, with a total of 572 sensing elements. A femoral component and insert of the same size and design were obtained from the manufacturer (DePuy Johnson & Johnson, Warsaw, IN). The insert test specimen was from the same polyethylene source and was subjected to the same sterilization method and packaging as the implanted insert. The components were mounted on a multiaxial testing machine (Force-5, AMTI, Watertown, MA). The Tekscan sensors were placed between the articulating surfaces of the medial and lateral compartments, and the contact stresses and contact area were measured with the implants aligned at multiple flexion angles (range, 0°–120°) and multiple axial loads (range, 1500–3600 N). A strong linear correlation was found between measured and predicted peak contact stresses ($R^2 > 0.9$, slope = 1.02, mean absolute error 6%; Fig. 2).

The comparison with the analytic Hertzian solution served to validate the contact algorithm utilized in MSC.MARC and to identify the optimal mesh density for a simplified geometry resembling unicompartmental tibiofemoral contact.

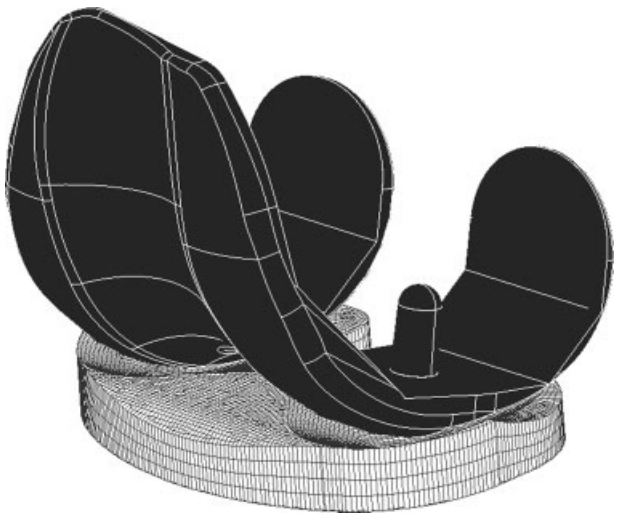

Figure 1. Surface geometries of the components were reconstructed by importing computer-aided design (CAD) models into a commercial FE program. The femoral component and tibial tray were modeled as rigid surfaces, while the tibial insert was modeled as a deformable body with elastoplastic properties.

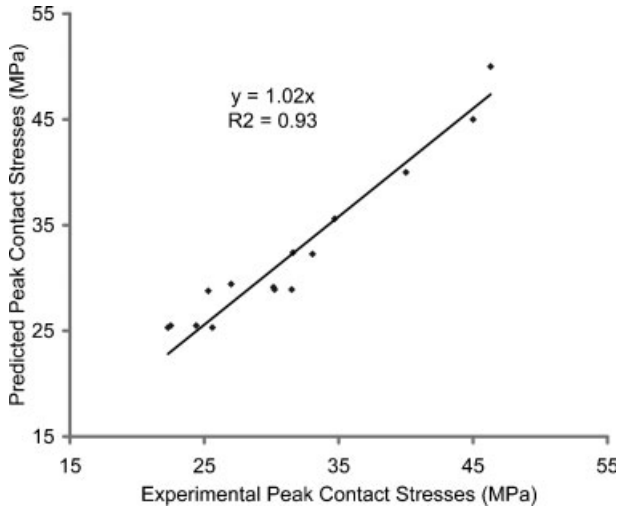

Figure 2. Experimentally measured peak contact stresses were compared against those predicted by the FE model under the same loading and kinematics conditions. The implants were aligned at multiple flexion angles (from 0° to 120°) and multiple axial loads (from 1500 to 3600 N). The strong linear correlation ($R^2 > 0.9$, slope = 1.02) validated the selection of the elastoplastic material model.

Differences between the geometry of the manufactured components and that used in the FE analysis can also affect contact stress calculations. The experimental data supported the choice of the elastoplastic model for polyethylene and validated the virtual geometry within the average absolute error of 6%.

Boundary Conditions

In the FE model, the femoral component was translated and rotated relative to the tibial component using fluoroscopically derived knee kinematics. The forces measured at the load cells in each quadrant of the instrumented tibial tray were used to calculate the magnitude and the location of the net compressive tibial load.[31] A vertical (axial) compressive load was applied at the appropriate location in the FE model. The tibial tray was free to rotate in adduction–abduction and to translate in the mediolateral direction to account for the high sensitivity of the contact analysis to potential errors in the fluoroscopic analysis in out-of-plane translations and rotations.[28] The tray was fixed in other degrees of freedom.

Average cycles were constructed from multiple cycles of synchronized knee kinematic and axial knee force experimental data. Details of the data synchronization and composition of average cycles were previously reported.[26] Three dynamic activities (fast gait, slow gait, and step-up) and two static deep flexion activities (kneeling and lunge) were simulated. The gait activities were performed on a treadmill, and the patient was allowed to rest his hands on the handlebars for safety. Step-up was conducted without external support. The deep flexion activities were conducted statically for several seconds and did not reflect dynamic muscle activity in moving into each position. For comparison of in vivo contact stresses with those generated during wear testing, we simulated contact using the ISO-recommended conditions for a displacement-controlled knee wear simulation[32] with a peak axial load of 2600 N, peak flexion of 58°, peak AP translation of 5.2 mm, and peak tibial rotation of 5.7°.

Contact Path Computation

The centroids of the medial and lateral contact patches were computed on the tibial and femoral articular surface for each increment over the entire gait cycle and ISO kinematic waveform (100 increments per cycle). The incremental change in centroid of the tibial contact was compared to that of the femoral contact. Pure rolling would result in the femoral and tibial contact centroids moving the same distance in the same direction. Pure sliding would result in a change in the tibial contact centroid without change in the femoral contact centroid or vice versa. During combined rolling and sliding, the difference between the tibial and femoral contact centroid changes would yield the sliding distance. This method of computing sliding distance was validated using analytical solutions of pure sliding, pure rolling, and combined sliding and rolling of a sphere of radius 14 mm on a flat surface. Total relative sliding distances per cycle for medial and lateral compartments were computed.

RESULTS

Walking

Peak and mean contact stresses during gait generally correlated with the axial load on the tibia. The following events were chosen for comparison: HS = peak load after heel-strike (first peak), TO = peak load before toe-off (second peak), and MS = the lowest load during mid-stance. Peak contact stresses, mean contact stresses, and contact areas for gait at two speeds were similar (Figs. 3 and 4). The ISO-loading waveform applies greater axial load (peak 2600 N) and therefore generated higher contact stresses. The peak contact stresses during ISO simulation were associated with the peak before toe-off (30 MPa) and were ~18% higher than peak in vivo contact stresses calculated for fast gait. The subject's weight was lower than that typically reported for TKA patients. Therefore, the axial load was scaled up to a subject with a bodyweight (BW) of 77 kg,[33] for which peak contacts stresses increased by 3.7% and 3.9% for the two peaks compared (just after heel-strike and before toe-off, respectively).

Stairs

Stair climbing is associated with higher knee flexion moments than level walking. In this subject, stair climbing generated higher contact forces (peak 3.5 BW) and peak contact stresses (Fig. 4). Maximum contact stresses were similar whether measured at peak knee force or at peak flexion angle. The center of pressure also moved posteriorly with flexion.

Deep Flexion

The subject had an excellent range of flexion; the fluoroscopically measured flexion angle between the femoral and tibial components was 133 (±0.4°) for kneeling and 132 (±0.2°) for lunge. During kneeling, most of the external ground reaction force was transmitted through the anterior surface of the upper tibia. During lunge, the ground reaction force was transmitted through the foot. The lunge generated modest contact forces (1.6 BW) relative to walking and stair

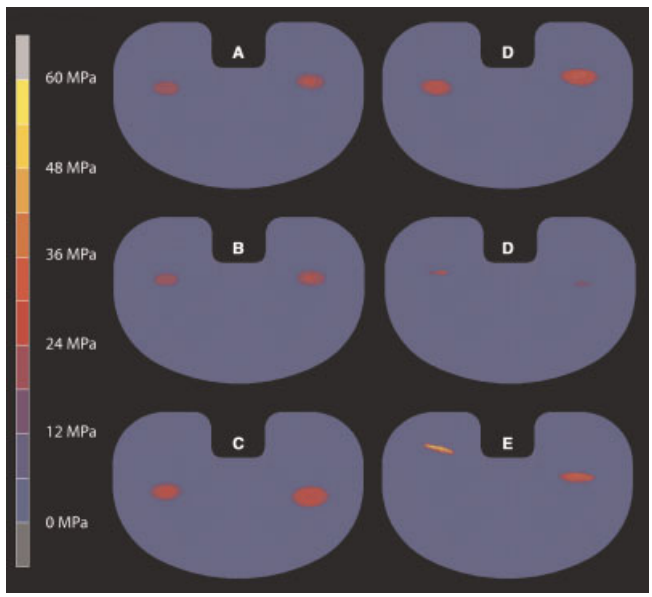

Figure 3. Contact stress contour map. (Left) Stresses generated at the first axial force peak after heel strike during: (A) fast gait, (B) slow gait, (C) ISO-loading conditions. (Right) Stresses generated during: (D) peak axial load during stair climbing, (E) kneeling, (F) lunging.

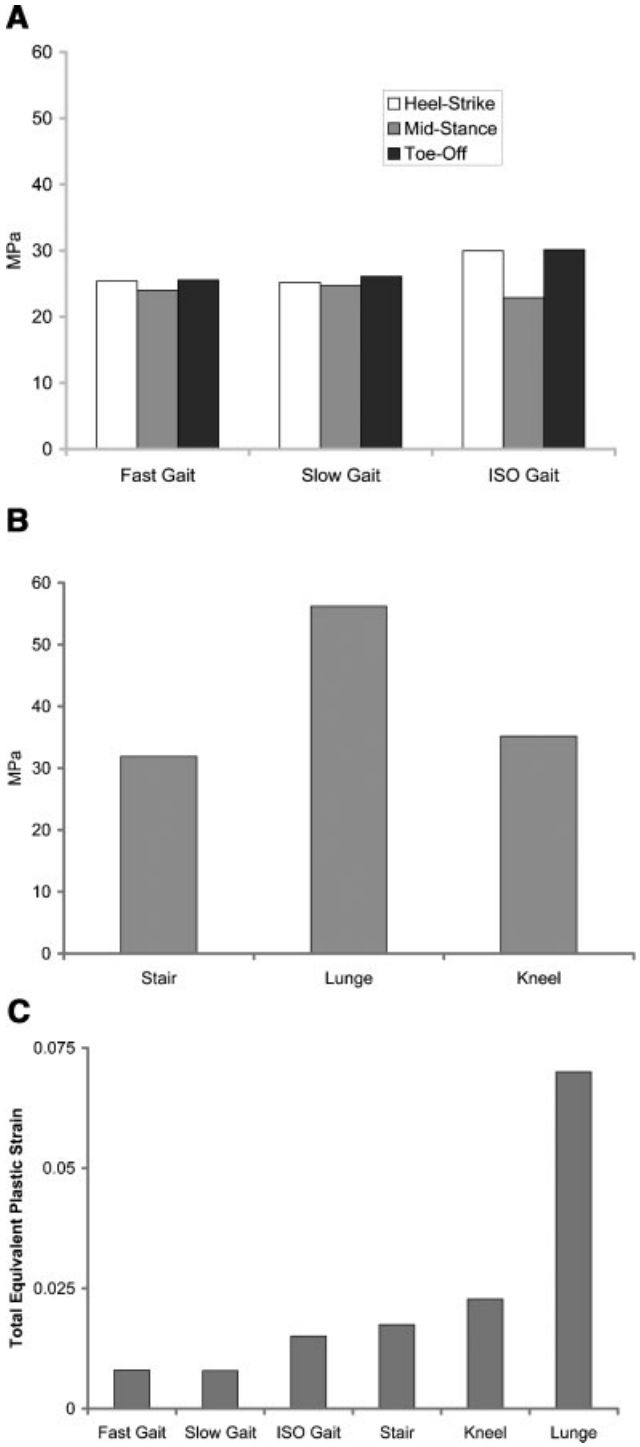

Figure 4. (A) Peak contact stresses generated during slow and fast gait were similar. The peaks generated during ISO knee simulator loading conditions were 18% higher. (B) Stair climbing generated higher contact stresses than gait. Both high flexion activities generated even higher stresses, with lunge generating the highest stresses. (C) Ranking activities by peak equivalent plastic strain did not change the order when compared to ranking based on peak contact stresses. However, the lunge was associated by far with the highest plastic equivalent strain.

climbing; however, peak contact stresses were the highest recorded (Fig. 4), due to the reduced contact area in deep flexion (<50% of the area calculated for stair climbing). Kneeling generated the lowest contact forces (0.3 BW) and contact area (29 mm^2) due to poor femorotibial contact in deep flexion. Despite low knee forces, kneeling produced peak contact stresses higher than those calculated for walking or stair climbing (Fig. 4).

Medial and Lateral Contact Stresses

Peak contact stresses in the medial compartment were higher during gait (fast and slow) and for the ISO-recommended knee loading and kinematic waveform (Table 1). Stair climbing also generated higher peak contact stresses medially. Kneeling and lunge generated markedly greater contact stresses in the lateral compartment.

Contact Path

The relative femorotibial sliding distance for the entire fast gait cycle for this patient was 61.6 mm in the medial compartment and 62.3 mm in the lateral, less than that calculated for ISO-recommended knee kinematics (71.4 and 83.7 mm, respectively). The sliding distance during stance was also lower (26.3 mm medially and 27.3 mm laterally compared to 31.8 and 38.7 mm, respectively, for the ISO kinematics).

Plastic Strain

Von Mises stresses are often used to estimate the potential for material damage.[2,34] Since the plasticity of the material model was a function of von Mises stresses, these stresses could not be used to assess potential for polyethylene damage. Therefore, we calculated the equivalent plastic strain near the articular surface of the insert as a measure of permanent deformation. As expected, the peak equivalent plastic strain was greater in those activities associated with higher peak contact stresses, but not in a linear fashion: the lunge generated peak equivalent plastic strain four times greater than that for other activities (Fig. 4C).

DISCUSSION

Stresses at the bearing surface are a major factor in polyethylene wear and fatigue, and affect the life of the implant. By accurately measuring tibiofemoral kinematics and forces in vivo, we were able to compute contact stresses generated during activities of daily living. Peak contact stresses and sliding distance can be used to rank activities by the potential for polyethylene wear and damage, and for comparison with knee wear simulation conditions.

Walking is generally considered an activity that subjects the prosthetic components to benign stresses in a well-aligned knee. Our data support this consensus since peak stresses were below those reported for the yield strength of polyethylene. Peak contact stresses for this subject were lower than those calculated using the ISO-recommended waveform primarily because of lower axial knee loads (1400 N in vivo vs. 2600 N ISO-recommended). In this subject, peak forces during walking were 2.2 BW, which in this was lower (68 Kg)

Table 1. Medial and Lateral Peak Contact Stresses

Activity	Event	Peak Lateral Contact Stresses (MPa)	Peak Medial Contact Stresses (MPa)
Fast gait	HS	24.20	25.40
Fast gait	MS	23.95	23.99
Fast gait	TO	23.29	25.55
ISO	HS	27.00	29.97
ISO	MS	20.99	22.88
ISO	TO	25.91	30.13
Slow gait	HS	23.32	25.19
Slow gait	MS	23.25	24.70
Slow gait	TO	22.61	26.09
Stairs	Peak tibial load	26.99	31.91
Kneel	Static pose	35.18	19.84
Lunge	Static pose	58.18	37.06

HS = peak load after heel-strike (first peak); TO = peak load before toe-off (second peak); MS = the lowest load during mid-stance.

than the mean bodyweight (~77 kg) reported for primary TKA patients.[33] However, even when the knee forces were scaled to represent a more typical patient's bodyweight, the peak contact stresses were lower than those calculated for the ISO-recommended waveform. Since benign wear is a function of contact stress and sliding distance, the increased sliding distance measured for the ISO condition indicates that the ISO-based wear simulation would generate a higher wear rate than that expected from the kinematic pattern of this subject. Treadmill walking with handlebar support may generate kinetics different from those generated during overground gait.

Stair climbing generated higher peak axial forces, which were most likely due to the high external flexion moment, since higher axial forces were associated with higher flexion angles. Peak axial forces during step-up were nearly 60% greater than during gait; peak contact stresses increased only 18%, most likely due to the inclusion of plasticity in the material model, which contributed to a 29% increase in contact area during stair climbing relative to gait.

In Western countries, the average knee flexion reported for successful TKA is 107° to 120°.[35–39] In Eastern and Middle Eastern countries, however, a greater degree of flexion is desired for activities such as squatting, kneeling, and sitting cross-legged that are important components of daily living. In Western populations, activities such as kneeling and gardening are also desirable but cannot always be achieved after TKA because of restricted knee flexion. These restrictions have led to design improvements targeted at increasing flexion. These designs have not been shown to actually increase postoperative range of motion;[40] however, one common change is to modify the articular geometry such that a reasonable contact area between the articular surfaces is maintained at high flexion, beyond the 130°–135° range of generic designs.[40] The goal is to better distribute the contact stresses in deep flexion. Our subject had flexion >130° and could kneel and perform the lunge. As expected, tibial forces were high during the lunge and thus contact stresses were also high. Conversely, tibial forces were remarkably low during kneeling, yet were associated with high contact stresses because of the small contact area. This finding indicates that so-called high flexion designs with increased contact area in deep flexion may reduce contact stresses in deep flexion in patients who achieve a high range of postoperative flexion and who participate in high flexion weight-bearing activities.

Due to the limited field of fluoroscopic view, only static kneeling poses were possible. In static poses, the effect of dynamic muscle contraction is minimal. We also measured tibial forces (without concomitant fluoroscopic motion analysis) during dynamic kneeling. Peak tibial forces as high as 2 BW were measured during dynamic single-limb loading kneeling. The subject did not habitually kneel or sit cross-legged; therefore, the forces measured may not apply to patient populations that habitually perform these activities. Nonetheless, the potential for high contact stresses during kneeling remains significant.

Peak contact stresses can be used to estimate potential for localized polyethylene damage, while average contact stresses are associated with potential for wear. Peak contact stresses generated during walking and stair climbing were similar. Lunge and kneeling generated the highest peak stresses and were therefore more likely to be associated with increased risk of damage. Plastic deformation under high stresses tends to increase contact area and may partially counteract substantial increases in contact stresses that would occur in an elastic material. Therefore, we also used equivalent plastic strain to determine potential for damage. Using plastic strain did not alter the ranking of activities in order of damage potential. However, the lunge generated dramatically higher peak plastic strain than the other activities. Conversely, peak plastic strain during kneeling was only slightly higher than that for stair climbing.

We obtained these results from one patient, so the values cannot be generalized to all TKA patients. Patient and design-related variability in contact conditions and polyethylene wear do not permit extrapolation to broader clinical outcomes. Knee forces were scaled up to estimate contact stresses if the patient's bodyweight was similar to the mean bodyweight reported for TKA patients. However, other individuals may generate forces equaling different multiples of bodyweight at the knee.[41] Direct comparison of our results with previous reports of contact stresses is difficult. Differences in contact stress predictions could be attributed to major differences in implant design, model formulation, material properties, and loading conditions. The use of in vivo data and careful validation of the FE model support our calculations. Only axial loads were measured in vivo. However, we have data to indicate that axial loads comprise >95% of the loads generated at the knee for the activities reported in this study.[42] Finally, these data were collected 8 months postoperatively. Ongoing recovery from surgery and increased strength with rehabilitation may alter load magnitude and distribution. Nonetheless, the changes with time are likely to be small.[23]

ACKNOWLEDGMENTS

Funds in partial support of this study were provided by OREF Grant 2609 and NIH R21 EB664581 to Darryl D. D'Lima, and by The Knee Society to Clifford W. Colwell, Jr. Partial support was provided by an NSF CAREER Award to Benjamin J. Fregly.

REFERENCES

1. Sharkey PF, Hozack WJ, Rothman RH, et al. 2002. Insall Award paper. Why are total knee arthroplasties failing today? Clin Orthop Relat Res 404:7–13.
2. Bartel DL, Rawlinson JJ, Burstein AH, et al. 1995. Stresses in polyethylene components of contemporary total knee replacements. Clin Orthop Relat Res 317:76–82.
3. Buechel FF, Pappas MJ, Makris G. 1991. Evaluation of contact stress in metal-backed patellar replacements. A predictor of survivorship. Clin Orthop Relat Res 273:190–197.
4. Collier JP, Mayor MB, Surprenant VA, et al. 1990. The biomechanical problems of polyethylene as a bearing surface. Clin Orthop Relat Res 261:107–113.
5. Weightman B, Light D. 1985. A comparison of RCH 1000 and Hi-Fax 1900 ultra-high molecular weight polyethylenes. Biomaterials 6:177–183.
6. Bartel DL, Bicknell VL, Wright TM. 1986. The effect of conformity, thickness, and material on stresses in ultra-high molecular weight components for total joint replacement. J Bone Joint Surg [Am] 68:1041–1051.
7. Hood RW, Wright TM, Burstein AH. 1983. Retrieval analysis of total knee prostheses: a method and its application to 48 total condylar prostheses. J Biomed Mater Res 17:829–842.
8. Kuster MS, Wood GA, Stachowiak GW, et al. 1997. Joint load considerations in total knee replacement. J Bone Joint Surg [Br] 79:109–113.
9. Szivek JA, Anderson PL, Benjamin JB. 1996. Average and peak contact stress distribution evaluation of total knee arthroplasties. J Arthroplasty 11:952–963.
10. Fukubayashi T, Kurosawa H. 1980. The contact area and pressure distribution pattern of the knee. A study of normal and osteoarthrotic knee joints. Acta Orthop Scand 51:871–879.
11. Kettelkamp DB, Jacobs AW. 1972. Tibiofemoral contact area—determination and implications. J Bone Joint Surg [Am] 54:349–356.
12. Peterson CD, Hillberry BM, Heck DA. 1988. Component wear of total knee prostheses using Ti-6A1-4V, titanium nitride coated Ti-6A1-4V, and cobalt-chromium-molybdenum femoral components. J Biomed Mater Res 22:887–903.
13. Fregly BJ, Sawyer WG, Harman MK, et al. 2005. Computational wear prediction of a total knee replacement from in vivo kinematics. J Biomech 38:305–314.
14. Knight LA, Pal S, Coleman JC, et al. 2007. Comparison of long-term numerical and experimental total knee replacement wear during simulated gait loading. J Biomech 40: 1550–1558.
15. Maxian TA, Brown TD, Pedersen DR, et al. 1996. The Frank Stinchfield Award. 3-Dimensional sliding/contact computational simulation of total hip wear. Clin Orthop Relat Res 333: 41–50.
16. Maxian TA, Brown TD, Pedersen DR, et al. 1997. Finite element analysis of acetabular wear. Validation, and backing and fixation effects. Clin Orthop Relat Res 344:111–117.
17. Patil S, Bergula A, Chen PC, et al. 2003. Polyethylene wear and acetabular component orientation. J Bone Joint Surg [Am] 85- (Suppl 4):56–63.
18. DesJardins JD, Walker PS, Haider H, et al. 2000. The use of a force-controlled dynamic knee simulator to quantify the mechanical performance of total knee replacement designs during functional activity. J Biomech 33:1231–1242.
19. Walker PS, Blunn GW, Perry JP, et al. 2000. Methodology for long-term wear testing of total knee replacements. Clin Orthop Relat Res 372:290–301.
20. D'Lima DD, Hermida JC, Chen PC, et al. 2001. Polyethylene wear and variations in knee kinematics. Clin Orthop Relat Res 392:124–130.
21. Muratoglu OK, Perinchief RS, Bragdon CR, et al. 2003. Metrology to quantify wear and creep of polyethylene tibial knee inserts. Clin Orthop Relat Res 410:155–164.
22. Collier JP, Mayor MB, McNamara JL, et al. 1991. Analysis of the failure of 122 polyethylene inserts from uncemented tibial knee components. Clin Orthop Relat Res 273:232–242.
23. D'Lima DD, Patil S, Steklov N, et al. 2005. The Chitranjan Ranawat Award: in vivo knee forces after total knee arthroplasty. Clin Orthop Relat Res 440:45–49.
24. D'Lima DD, Patil S, Steklov N, et al. 2006. Tibial forces measured in vivo after total knee arthroplasty. J Arthroplasty 21:255–262.
25. D'Lima DD, Townsend CP, Arms SW, et al. 2005. An implantable telemetry device to measure intra-articular tibial forces. J Biomech 38:299–304.
26. Zhao D, Banks SA, D'Lima DD, et al. 2007. In vivo medial and lateral tibial loads during dynamic and high flexion activities. J Orthop Res 25:593–602.
27. Zhao D, Banks SA, Mitchell KH, et al. 2007. Correlation between the knee adduction torque and medial contact force for a variety of gait patterns. J Orthop Res 25:789–797.
28. Banks SA, Hodge WA. 1996. Accurate measurement of three-dimensional knee replacement kinematics using single-plane fluoroscopy. IEEE Trans Biomed Eng 43:638–649.
29. Fischer-Cripps AC. 2000. Introduction to contact mechanics. New York: Springer-Verlag.
30. Kurtz SM, Pruitt L, Jewett CW, et al. 1998. The yielding, plastic flow, and fracture behavior of ultra-high molecular weight polyethylene used in total joint replacements. Biomaterials 19:1989–2003.

31. Kaufman KR, Kovacevic N, Irby SE, et al. 1996. Instrumented implant for measuring tibiofemoral forces. J Biomech 29:667–671.
32. International Standards Organization. 2000. Standard number 14243-3. Implants for surgery; wear of total knee joint prostheses. Part 3: loading and displacement parameters for wear-testing machines with displacement control and corresponding environmental conditions for test. Geneva, Switzerland: ISO.
33. Rodricks DJ, Patil S, Pulido P, et al. 2007. Press-fit condylar design total knee arthroplasty. Fourteen to seventeen-year follow-up. J Bone Joint Surg [Am] 89:89–95.
34. Elbert K, Bartel D, Wright T. 1995. The effect of conformity on stresses in dome-shaped polyethylene patellar components. Clin Orthop Relat Res 317:71–75.
35. Anouchi YS, McShane M, Kelly F Jr, et al. 1996. Range of motion in total knee replacement. Clin Orthop Relat Res 331:87–92.
36. Buehler KO, Venn-Watson E, D'Lima DD, et al. 2000. The press-fit condylar total knee system: 8- to 10-year results with a posterior cruciate-retaining design. J Arthroplasty 15:698–701.
37. Lee DC, Kim DH, Scott RD, et al. 1998. Intraoperative flexion against gravity as an indication of ultimate range of motion in individual cases after total knee arthroplasty. J Arthroplasty 13:500–503.
38. Mahoney OM, McClung CD, de la Rosa MA, et al. 2002. The effect of total knee arthroplasty design on extensor mechanism function. J Arthroplasty 17:416–421.
39. Ritter MA, Harty LD, Davis KE, et al. 2003. Predicting range of motion after total knee arthroplasty. Clustering, log-linear regression, and regression tree analysis. J Bone Joint Surg [Am] 85-A:1278–1285.
40. Kim YH, Sohn KS, Kim JS. 2005. Range of motion of standard and high-flexion posterior stabilized total knee prostheses. A prospective, randomized study. J Bone Joint Surg [Am] 87: 1470–1475.
41. Taylor WR, Heller MO, Bergmann G, et al. 2004. Tibiofemoral loading during human gait and stair climbing. J Orthop Res 22:625–632.
42. D'Lima DD, Patil S, Steklov N, et al. 2007. In vivo knee moments and shear after total knee arthroplasty. J Biomech 40:S11–S17.